Proceedings Paper:
Lungu, A. orcid.org/0000-0002-4531-2791, Swift, A.J. orcid.org/0000-0002-8772-409X, Danciu, A.S. orcid.org/0009-0002-0917-6216 et al. (3 more authors) (2025) AI-based 3D segmentation of pulmonary vasculature of CTEPH patients. In: Vlad, S. and Roman, N.M., (eds.) 9th International Conference on Advancements of Medicine and Health Care Through Technology. MEDITECH 2024 International Conference on Advancements of Medicine and Health Care Through Technology, 30 Sep - 02 Oct 2024, Cluj-Napoca, Romania. IFMBE Proceedings, 130 . Springer Nature Switzerland , pp. 107-114. ISBN: 9783031956706 ISSN: 1680-0737 EISSN: 1433-9277

https://doi.org/10.1007/978-3-031-95671-3_13

AI-based 3D Segmentation of Pulmonary Vasculature of CTEPH patients

Angela Lungu[1[0000-0002-4531-2791]], Andrew J. Swift[2[0000-0002-8772-409X]], Alina S. Danciu[1[0009-0002-0917-6216]], Michael Sharkey[2[0000-0001-9851-0014]], Rod D. Hose[2], Maciej Malawski[3[0000-0001-6005-0243]]

[1] Technical University of Cluj-Napoca, Cluj-Napoca, RO
[2] University of Sheffield, Sheffield, UK
[3] Sano Centre for Computational Medicine, Krakow, PL

angela.lungu@ethm.utcluj.ro

Abstract. Chronic thromboembolic pulmonary hypertension (CTEPH) presents challenges for pulmonary artery segmentation due to vascular remodeling, stenosis, and obstructions. This study evaluates a 7-layer dilated convolutional neural network (CNN) with Tversky loss, applied to computed tomography angiography (CTA) images that were preprocessed with image enhancement techniques. The model achieved a Dice score of 0.792 on non-CTEPH data but scored 0.693 on CTEPH data, reflecting the challenges of manual segmentation, where smaller branches are often missed. While the results align with other research, advanced 3D CNN models have shown higher accuracy. Future work should refine ground truth data and explore 3D models to better capture CTEPH-specific complexities.

Keywords: 3D segmentation, AI, CTEPH.

1 Introduction

Pulmonary hypertension is a clinical condition characterised by an increase in the mean pulmonary pressure >20 mmHg, measured at right heart catheterisation. Imaging modalities such as magnetic resonance (MRI) or computed tomography (CT) play a crucial role during the diagnosis, assessment, and patient follow-up of PH patients [1]. Over the past two decades, tools based on computer modelling and artificial intelligence [2] have emerged, supporting the clinical decision-making process.

Among these tools, blood flow hemodynamics simulations could provide a deeper understanding of pressure and flow distribution, and they could be used to predict the changes that may occur after surgical intervention [3], as it is the case in chronic thromboembolic hypertension (CTEPH). Often, the development of personalised models of the pulmonary vasculature relies on quick and sensible image segmentation and geometry reconstruction. Various research teams [4-8] have proposed AI-based tools for detailed pulmonary arterial segmentation and reconstruction, showing high agreement

with manually segmented ground truth. However, these methods are not focused on CTEPH patients, who present significant arterial remodeling, stenosis, webs, and bands [9], complicating the task.

This paper evaluates whether a 2D convolutional neural network, supported by image processing techniques, can offer accurate pulmonary arterial tree segmentation in CTEPH.

2 Materials and methods

2.1 Datasets

The proposed segmentation method was developed using two image datasets. The first, referred to as SheffCTEPH has CTA images from 14 CTEPH patients, collected at the Sheffield Pulmonary Disease Unit. All patients provided written consent for data collection.

The images have matrix dimensions of 512x512 pixels, with stack heights ranging from 905 to 1256 slices per patient. The mean in-plane resolution is 0.72 mm/pixel, and the average slice thickness is 0.625 mm.

The second dataset consists of CTA volumetric images and corresponding masks from 100 subjects, available through the PARSE challenge [7]. The stack height of these images varies between 228 to 376 slices. Since no information on the clinical conditions of these subjects is available, this dataset is referred to as noCTEPH.

2.2 Generation of the ground truth masks

The images were segmented using the MIMICS software package (www.materialise.com). 3D geometry rendering, visualisation and comparison of cases was performed with 3D Slicer (www.slicer.org/). All the 2D image processing as well as AI model implementation and evaluation were performed in MATLAB R2023b (www.mathworks.com), using various built-in toolboxes, including the Image Processing Toolbox and Deep Learning Toolbox.

It is important to note that the masks for the SheffCTEPH dataset were generated from 3D reconstructed geometries, which were cleaned and smoothed for haemodynamic model-based analysis. Due to this process, the level of detail at the branch level was reduced for some CTEPH patients.

2.3 Image preprocessing

All the images went through several preprocessing steps including contrast enhancement, pixel values scaling and normalisation, image cropping and resizing. The image contrast enhancement was achieved after clipping the pixel values between -800 and 500 Hounsfield units (HU), followed by min-max pixel scaling and normalisation in the [0, 1] interval.

Cropping all the volumes with a rectangle that includes the structures delimited by the outside lungs border was further applied. The creation of this region of interest (ROI) included: (i) binarisation of the volume central slice with an optimal threshold value chosen based on the histogram using the Otsu method [10], (ii) cropping the grayscale image with a rectangle that frames the object with the largest perimeter in the binary image, (iii) binarising the newly cropped grayscale image and create its negative to outline the lungs, (iv) retaining the two lungs from the complement image, (v) cropping the lung mask with a rectangle that fully encloses them, and (vi) cropping all images in the volume according to the new coordinates. For each data volume, the cropping coordinates were determined based on the image corresponding to the middle slice. Finally, all the images were resized at 512 x 512 and individually saved as .png files. Figure 1 shows the 2D image preprocessing steps illustrated on a slice.

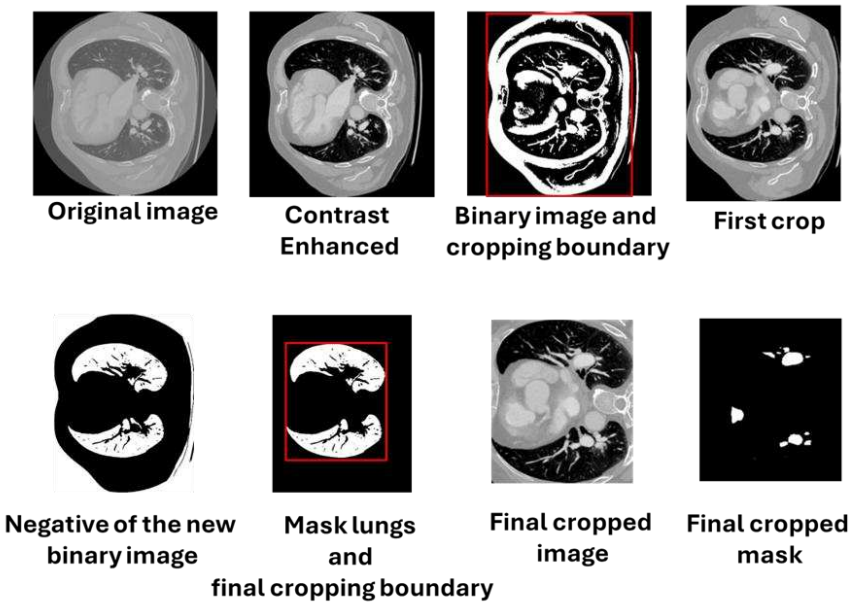

Fig. 1. Images preprocessing steps

2.4 AI based images segmentation

For the task of image segmentation a dilated convolutional neural network (DCNN)[11] architecture was used. The dilated convolutions allow the network to capture features at multiple scales, which is essential for detecting the fine details of small arteries while also understanding the broader context required for segmenting larger arteries, both being present in the CT images of the pulmonary arteries. By expanding the receptive field without reducing spatial resolution, the network can accurately differentiate small, intricate vessels alongside larger structures, making it well-suited for this type of medical imaging task.

The network's first layer processes grayscale images with a 512x512 matrix size on a single channel, followed by six convolutional blocks. Each block includes a convolutional layer with 64 filters (3x3), batch normalization to stabilize training, and ReLU activation for non-linearity. To capture features at different scales, dilation factors (1, 2, 4, 8, 16, 32) were applied, increasing with network depth. The final 1x1 convolutional layer reduces the number of channels to match the number of classes, preparing the output for the softmax layer to generate pixel-wise class probabilities.

The training was carried out using the Adam optimizer, with a learning rate of 1e-4, for 100 epochs, in mini-batches of 4 images. The Tversky loss function [12], with α=0.3 and β=0.7, chosen empirically after trying several configurations, was used to penalize false negative predictions (white pixels defined as background) in an attempt to compensate for the class imbalance.

The dataset was split into 70% for training, 10% for validation, and 20% for testing, ensuring that no .png images from the same subject appeared in more than one set to avoid data leakage and improve model generalization.

A final image post-processing step, based on simple morphological operations such as opening (using a structural disk element with a radius of 1) and hole filling, was applied to the test set masks before evaluating the final results.

3 Results and discussions

The results were evaluated on the entire test set, as well as separately on each type of images to better underline the challenges in the CTEPH cohort. Figure 2 shows a comparison between the ground truth mask and the mask estimated by the trained neural network for images from both categories (CTEPH and noCTEPH). Generally, the network successfully identifies the large arteries, but the agreement with smaller blood vessels is weaker, especially for the SheffCTEPH data.

Table 1. Evaluation metrics computed on the test set

		JACCARD	DICE	ACCURACY
NoCTEPH	artery	0.656	0.792	0.897
	background	0.995	0.997	0.996
SheffCTEPH	artery	0.530	0.693	0.835
	background	0.992	0.996	0.994
NoCTEPH+SheffCTEPH	artery	0.557	0.715	0.850
	background	0.993	0.996	0.994

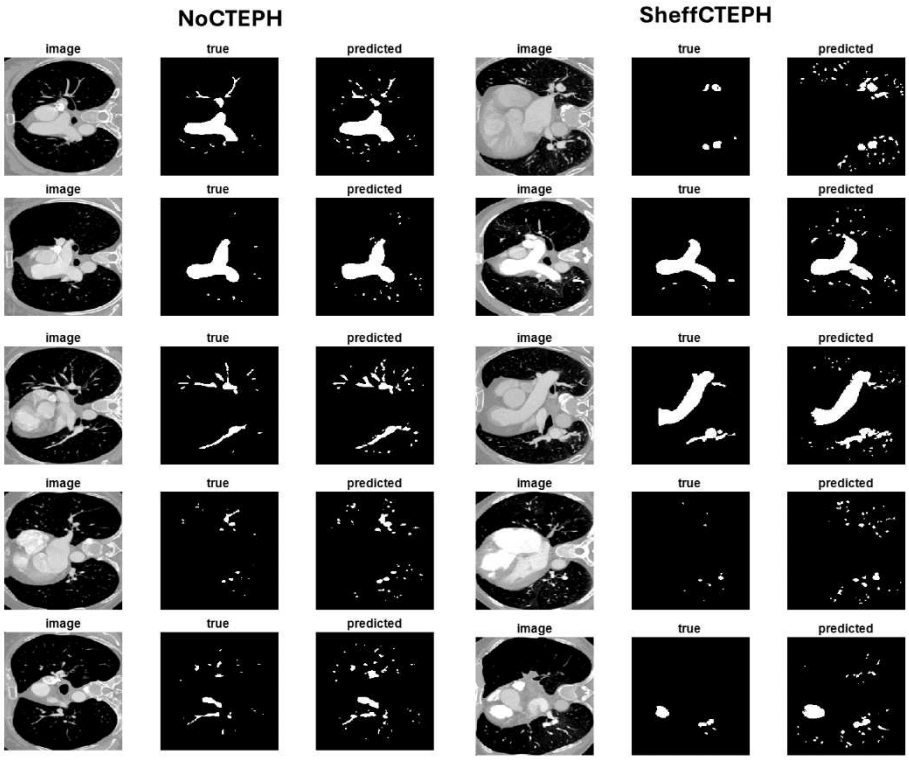

Fig. 2. Examples of 2D images from the test sets with corresponding ground truth and predicted masks

Examples of reconstructed geometry from the 2D segmented masks are shown in Figure 3 and 4. It can readily be noticed that while the AI-based segmentation model provides results closer to those of the human expert for the noCTEPH set, it predicts more arterial vessels than the ground truth in CTEPH cases. The CTEPH examples in Figure 4 highlight both the tortuosity of the vascular tree in these patients and the arterial path obstruction in the proximal vessels.

The qualitative results were supported by the quantitative data presented in Table 1, expressed as the mean Dice and Jaccard indices [13] as well as accuracy, based on binary pixel classification across all slices.

As it can be noticed, the highest artery Dice score of 0.792 was achieved for the noCTEPH set, while the lowest score of 0.693 was recorded for the CTEPH set. The mixed test set scored 0.715. The lower score for the CTEPH cases is influenced by the ground truth segmentation, which missed unconnected branches that were not identified during manual segmentation.

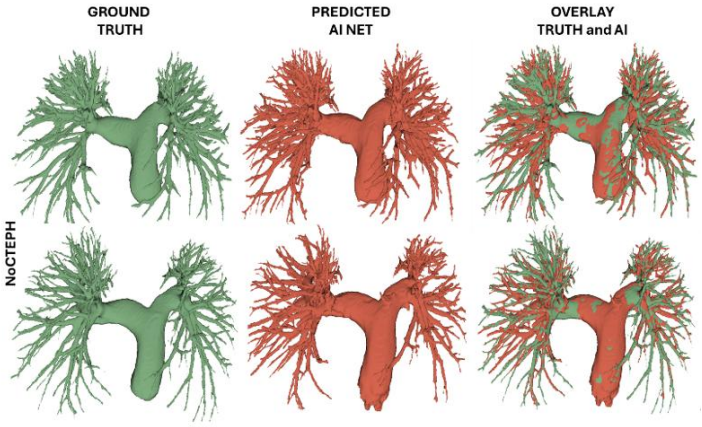

Fig. 3. Geometry reconstructions of the masks from the noCTEPH test set

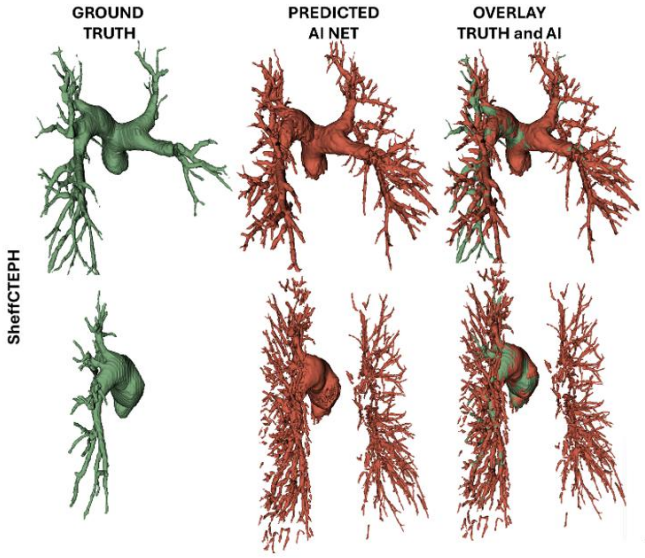

Fig. 4. Geometry reconstructions of the masks from the SheffCTEPH test set

The results for the entire set are in the range of those reported by the 25 teams participating in the Parse Grand challenge [7], where the highest score was 0.7969. On the same Parse dataset, L. Lou. et. al [4] reported with their 2D-CNN a mean dice score of 0.7816. Superior results were showed for the more complex, 3D CNN, as it is the case of M. Zulfiqar et. al [6] or J. Han et. al [5], reporting mean dice scores of 0.8775 and 0.8659, respectively. It is important to note that these results were obtained from generic lung CTA images, with no mention of CTEPH cases. A few research groups reported results on CTEPH data, such as H. Suzuki et. al [14] who focused on main

pulmonary artery segmentation, showing a dice score of 0.968, or Kim et. al. [15] who presented a deep learning-based pulmonary arterial tree segmentations in CTEPH but did not provide evaluation scores. In contrast, our research utilizes specialized image enhancement techniques and a CNN modified with Tversky loss to specifically address the unique challenges of segmenting pulmonary arteries in CTEPH patients—a domain that has been relatively underexplored in existing studies. This approach not only provides critical insights but also achieves significant improvements in segmentation accuracy for this particularly complex patient group.

4 Conclusions

This study explored the use of a 7-layer dilated convolutional network with Tversky loss for segmenting pulmonary arteries in 2D CTA images. Image enhancement techniques were applied during preprocessing to support the segmentation of arteries in both CTEPH and non-CTEPH cases. The model achieved a Dice score of 0.792 in non-CTEPH cases but struggled in CTEPH cases, with a lower score of 0.693, likely due to missing details in the ground truth caused by complex vascular alterations typical of CTEPH. While the performance aligns with similar 2D CNN-based studies, more advanced 3D models and refined segmentation processes could improve accuracy and clinical relevance in CTEPH cases.

Conflict of Interest statement

The authors have no conflict of interest to declare.

Acknowledgments

This work was supported through the research project PN-III-P1-1.1-PD-2021-0601. The authors would like to thank Sheffield Pulmonary Vascular Disease Unit, UK for providing the CTA image data of CTEPH patients used in this study.

This project has received funding from the European Union's Horizon 2020 research and innovation programme under grant agreement No 857533. The publication was created within the project of the Minister of Science and Higher Education "Support for the activity of Centers of Excellence established in Poland under Horizon 2020" on the basis of the contract number MEiN/2023/DIR/3796 and is supported by Sano project carried out within the International Research Agendas programme of the Foundation for Polish Science, co-financed by the European Union under the European Regional Development Fund.

References

1. Humbert, M., et al., *2022 ESC/ERS Guidelines for the diagnosis and treatment of pulmonary hypertension.* Eur Heart J, 2022. **43**(38): p. 3618-3731.

2. Lungu, A., et al., *Diagnosis of pulmonary hypertension from magnetic resonance imaging–based computational models and decision tree analysis.* Pulmonary Circulation, 2016. **6**(2): p. 181-190.
3. Colebank, M.J., et al., *A multiscale model of vascular function in chronic thromboembolic pulmonary hypertension.* Am J Physiol Heart Circ Physiol, 2021. **321**(2): p. H318-h338.
4. Lou, L., et al., *A detail-oriented super-2D network for pulmonary artery segmentation.* Biomedical Signal Processing and Control, 2024. **93**: p. 106183.
5. Han, J., et al., *3D pulmonary vessel segmentation based on improved residual attention u-net.* Medicine in Novel Technology and Devices, 2023. **20**: p. 100268.
6. Zulfiqar, M., et al., *DRU-Net: Pulmonary Artery Segmentation via Dense Residual U-Network with Hybrid Loss Function.* Sensors, 2023. **23**(12): p. 5427.
7. Luo, G., et al., *Efficient automatic segmentation for multi-level pulmonary arteries: The PARSE challenge.* arXiv preprint arXiv:2304.03708, 2023.
8. Wu, Y., et al., *Transformer-based 3D U-Net for pulmonary vessel segmentation and artery-vein separation from CT images.* Med Biol Eng Comput, 2023. **61**(10): p. 2649-2663.
9. Shahin, Y., et al., *Quantitative CT Evaluation of Small Pulmonary Vessels Has Functional and Prognostic Value in Pulmonary Hypertension.* Radiology, 2022. **305**(2): p. 431-440.
10. Xu, X., et al., *Characteristic analysis of Otsu threshold and its applications.* Pattern Recognition Letters, 2011. **32**(7): p. 956-961.
11. Yu, F. and V. Koltun *Multi-Scale Context Aggregation by Dilated Convolutions*. 2015. arXiv:1511.07122 DOI: 10.48550/arXiv.1511.07122.
12. Jadon, S. and IEEE. *A survey of loss functions for semantic segmentation*. in *2020 IEEE CONFERENCE ON COMPUTATIONAL INTELLIGENCE IN BIOINFORMATICS AND COMPUTATIONAL BIOLOGY (CIBCB)*. 2020.
13. Taha, A.A. and A. Hanbury, *Metrics for evaluating 3D medical image segmentation: analysis, selection, and tool.* BMC Med Imaging, 2015. **15**: p. 29.
14. Suzuki, H., et al., *Aorta and main pulmonary artery segmentation using stacked U-Net and localization on non-contrast-enhanced computed tomography images.* Medical Physics, 2024. **51**(2): p. 1232-1243.
15. Kim, J., et al., *Abstract 17842: 3D Visualization and Quantitative Assessment of the Pulmonary Arteries on CT Using Deep Learning Segmentation.* Circulation, 2023. **148**(Suppl_1): p. A17842-A17842.